CONTINUOUS ON-CHIP MICROPUMPING THROUGH A MICRONEEDLE

Jeffrey D. Zahn[1,2], Ajay A. Deshmukh[1,3], Albert P. Pisano[1,3] and Dorian Liepmann[1,2,3]
[1]Berkeley Sensor and Actuator Center, [2]Department of Bioengineering and [3]Department of Mechanical Engineering
497 Cory Hall, University of California at Berkeley, Berkeley, CA 94720-1774

ABSTRACT

Microneedles are promising microfabricated devices for minimally invasive drug delivery applications. Microneedles can be integrated into a variety of devices. However, any portable drug delivery device with integrated microneedles will need an equally compact means to deliver the therapeutics. This work presents microneedles integrated with an on-chip MEMS positive displacement micropump for continuous drug delivery applications. The generation and collapse of thermally generated bubbles with flow rectified by directional check valves are used to achieve net pumping. Visualization methods have observed net flow rates of water out of a microneedle at approximately 1.0 nl/s with a pressure of 3.9 kPa. In addition, continuous pumping was achieved for more than 6 hours. The heaters operated for over 18 hours (15,000 cycles) without failing.

INTRODUCTION

In modern medical applications, there is a need for very small hypodermic needles that are economical to fabricate. Currently the smallest needles available, stainless steel 30 gauge needles, have a 305 μm outer diameter with a wall thickness of 76 μm. Traditional machining methods make it unfeasible to create needles with a diameter less than 300 μm. Microneedles on the other hand can be almost any size and geometry since they are defined lithographically.

Microneedles [1-3] reduce insertion pain and tissue damage in patients. They are extremely attractive for delivering therapeutics in a portable intravenous drip fashion, such as the continuous delivery of insulin to a diabetic patient. The microneedles would be integrated into a short-term drug delivery device capable of delivering therapeutics transdermally for about 24 hours. Continuous drug delivery increases drug effectiveness and lowers side effects for a large range of therapeutics. However, this device will need a compact means to deliver the correct drug dosages. Microfabrication technology allows tighter control over physical parameters (flow rates and pressure, for example) [4-7] for the precise delivery of concentrated drug solutions in order to meet dosage specifications. By integrating microneedles with planar micropumps [4,5], very tight control over injection flow rates at given drug concentrations can be achieved. In addition, a more concentrated drug solution may be used at very low flow rates and administrated as needed by the patient. Thus, the drug concentration in the body may be controlled, to achieve either a constant or time varying drug concentration profile in the body.

In addition, such a device can also be used for sample collection for biological analysis. The pumps may be used for fluid extraction through the microneedle simply by reversing the valve directions so the net pumping is from the body into the device rather than out from the device to the body. Thus, an integrated device could be fabricated to determine glucose levels for diabetics. In this scenario, one microneedle/pump system could sample interstitial fluid to determine glucose level while a second pump could deliver insulin in a controlled manner as needed by the patient.

THEORY AND DESIGN

Planar micropumps have the advantage of being easily integrated with other planar fluidic components. The pumps consist of a bubble chamber and two check valves [5]. Vapor bubbles are created by polysilicon resistors on quartz which act as heaters. Vapor bubbles (literally steam bubbles) are generated by the heat dissipated when an electric current is run through the resistor. When the electric current is interrupted, the vapor will recondense and the bubble will collapse. When a vapor bubble is created, it acts as a piston and drives fluid out of the pumping chamber. The check valves are free floating silicon pieces that are moved by viscous drag. Flow in a positive direction will open the valve, whereas flow in the opposite direction will drag the valve closed. By cycling bubble generation and collapse, a net pumping action occurs. Microneedles may be integrated by adding them to the fluid flow path (Fig. 1).

Microneedles are formed by a polysilicon molding process. The shape of the needle is defined lithographically. Therefore, many features may be incorporated into the microneedles. For ease of handling some microneedles were designed with a large base that may be placed into an etched cavity to couple the needle flow path to that of the micropump.

FABRICATION

Microneedles are fabricated using a polysilicon micromolding method as previously described [1,2]. A double polished silicon is used as a starting material as shown in Fig. 2. The wafer is wet oxidized at 1000°C to grow 1 μm of thermal oxide. The needle shapes are patterned using standard lithographic techniques and the patterned oxide is etched with reactive ion etching (RIE). The wafer is coated with 0.3 μm of low-pressure chemical vapor deposition (LPCVD) low stress silicon nitride. The backside of the wafer is aligned and patterned to the needle design. The silicon nitride and oxide films are then etched away using RIE. Afterwards, the through holes are etched with potassium hydroxide (KOH). The nitride is removed in phosphoric acid at 175°C. The needle mold is etched using deep reactive ion etching (DRIE). The wafer is then wet oxidized at 1000°C to decrease surface roughness. Afterwards 2 m of phosphosilicate glass (PSG) is deposited onto the mold wafer. A second bare silicon

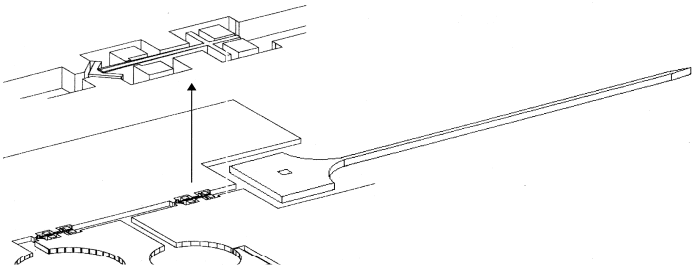

Figure 1. *Schematic of an integrated micropump/microneedle device. The top shows a closeup of a planar microvalve.*

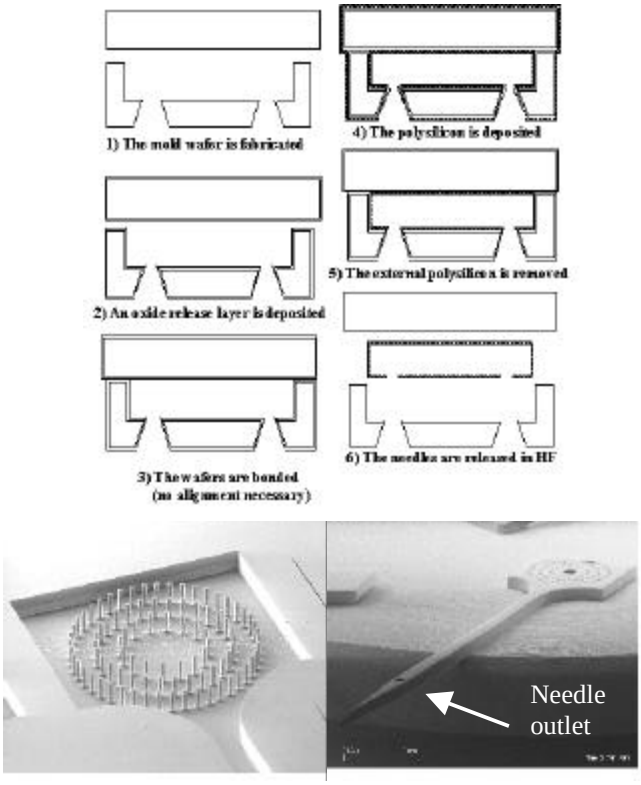

Figure 2. *(Top)Microneedle fabrication process flow. (Bottom Left) SEM of a microneedle mold. (Bottom Right) SEM of a representative microneedle.*

wafer is coated with 2 μm of PSG. These two wafers are pressure bonded at 1000°C in a N_2 atmosphere. After bonding, 4 μm of polysilicon is deposited onto the mold wafers at 580°C and then annealed at 1000°C. The deposition and annealing process is repeated until the desired thickness is reached, typically 15-20 μm. After deposition, the external polysilicon is removed by RIE. The needles are then released in concentrated HF overnight.

The pump is made of Silicon on Insulator (SOI) and quartz dice. The SOI wafer has a 2 μm thick buried oxide layer and a 75 μm device layer. Two sequential deep reactive ion etches (DRIE) are performed; the first going all the way through the wafer to form through holes, while the second going only through the device layer to create the channels. A 1.3 μm thick wet oxide layer provides the mask for the second etch while a layer of 9.5 μm thick photoresist over the oxide serves as the mask for the first etch. After the DRIE processes, the valves are almost completely freed from the substrate in 5:1 BHF. They are then placed in H_2O_2 to generate a thin oxide layer on the bottom of the valve. Afterwards, a probe tip is used to gently free the valves (Fig. 3). The quartz wafer has 3000 Å n^+ doped polysilicon and 1000 Å sputtered platinum applied. The layers, after being patterned into heaters, are passivated with silicon oxide and/or silicon nitride, leaving openings for the electrical connections. A low viscosity epoxy (Epotek 301) is spun on at 10,000 rpm. The two dies are then 'flip-chipped', with pressures of between 100 – 300 kPa per 1 cm^2 die. The epoxy bonds and seals the dies but also traps the valve bodies. In Fig. 4, the covering die has been bonded on top and an epoxy layer fills the gap between the two surfaces.

An oxygen plasma (200 W in 600 mtorr of O2) is used to remove the epoxy in the fluid channels. Through holes allow the plasma to access the fluid channels. The oxygen first removes the epoxy on the top of the channels and then moves slowly outward from the channel. The plasma etching is timed to free the valves without penetrating far from the channel edge. The valves are freed, but sufficient epoxy remains outside the channels to bond and seal the device.

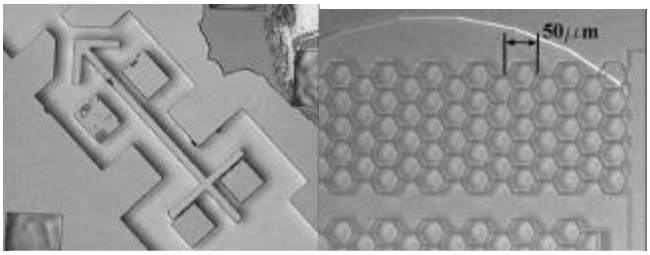

Figure 3. *(Left) A microfluidic checkvalve. (Right) Fabricated and assembled crack resistant polysilicon heater.*

In Fig. 4 is shown the edge of the epoxy layer. The epoxy has been etched farther above the channel than below it, possibly due to non-uniformity in the epoxy layer. Once the valves are free, the devices are placed in an H_2O_2 and surfactant ultrasound bath in order to create an oxide layer surrounding the valve bodies.

A descriptive cross section is shown in Fig. 5. It does not correspond to any actual cross section in the device but is a combination of the heater and valve structures. A seat for the microneedle is defined using DRIE. The microneedle is placed into the seat and sealed using a two-part epoxy.

EXPERIMENTAL DETAILS

Successful integration of microneedles with micropumps has been accomplished. As shown in Fig. 6, a working micropump has been developed. The tracking bubble in the series of pictures can be used to visualize fluid flow. The tracking bubble is stationary until the heater is activated. Subsequently, the fluid starts moving and travels to the outlet. The fluid velocity in the channel is not constant since the bubble generation and collapse creates a time oscillating flow profile. The velocity of the bubble shown is estimated to be 15 mm/sec, which is a peak velocity for the pump.

Once dies are assembled they are wirebonded onto a circuitboard package to allow easy application of electrical power to the heaters. The heaters can create vapor bubbles at different rates by varying the heater voltage and time applied. In the experiment, various bubble creation/collapse rates have been achieved through a computer control mechanism. A power supply is set to a given potential, and supplied to the device through a relay. The relay is actuated by a HP-VEE output through a D/A circuitboard. The HP-VEE interface controls the time power is supplied to the device, while the power supply controls the voltage.

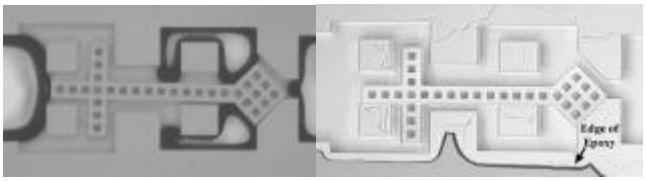

Figure 4. *(Left) Check Valve after epoxy bonding and before ashing. (Right) Same valve after ashing.*

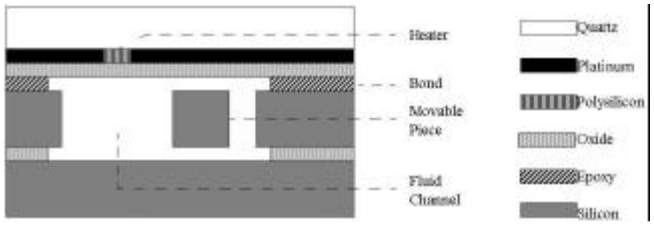

Figure 5. *Description cross section of the device*

In figure 7 is shown how the radius of curvature of water at but surface tension from the outlet free surface constrains fluid from pumping out and the radius of curvature at the outlet increases. Then as the vapor bubble collapses, it pulls fluid back into the needle before the microvalve is completely seated. This causes the outlet fluid surface to become concave until pressure is allowed to equilibrate again and the outlet surface returns to its convex conformation. At the outlet free surface no net pumping is seen, since the surface tension from the small outlet radius of curvature opposes the pressure generated by the vapor bubble. The radius of curvature at the outlet is approximately the same as the channel depth (37 μm). Therefore the pressure generated in the vapor bubble (approximately 3.9 kPa given by $2\sigma/r$ where σ is the surface tension and r is the minimum bubble radius of curvature) is opposed by the outlet free surface and the vapor bubble growth is constrained, so no net pumping is seen.

When surface tension is diminished by allowing a drop of fluid to collect around the needle end then a net pumping is seen. The most successful micropumping was with the application of 40 V to the heater. The heater was on for 2 seconds and off for 3 seconds to allow bubble collapse. This corresponds to a power dissipation of 0.5 W. Under these conditions continuous pumping was observed for a period of 6 hours. The device was left actuating over night. Upon returning the heater was still functioning over the entire 15,000 cycles. However, pumping had stopped sometime during this period due to evaporation at the outlet. Consequently, the pressure opposing the flow due to the free surface of water at the outlet had risen and precluded pumping as previously described. However, with the application of an external pressure to overcome the surface tension at the outlet, pumping resumed. The vapor bubble creation/collapse cycle had been continuously performed for 18 hours straight. The authors hypothesize that pumping would have continued for a full 18 hours had this free surface not opposed the pumping. However, flow visualization to confirm pumping was extremely difficult when the needle was submerged under water to remove the free surface.

As shown in Figure 8, a net pumping is seen when the flow is visualized by fluorescent beads. When power is not applied a background flow of approximately 0.15 nl/s is present due to a head pressure from fluid in the filling lines. However, once the heater is turned on, a net pumping of 1 nl/s can be observed. Flow rates are estimated by estimating the volume flux out of the needle using the beads. The microscope objective has a depth of field of 5 μm, and the needle outlet is 70 X 70 μm2. Thus, when the pump is off the beads can be recorded and seen to stay in focus for 0.16 sec. The bead velocity is therefore

v = (depth of focus)/(time in focus). [1]

A flow rate can be estimated as

Q = (outlet area)*(bead velocity). [2]

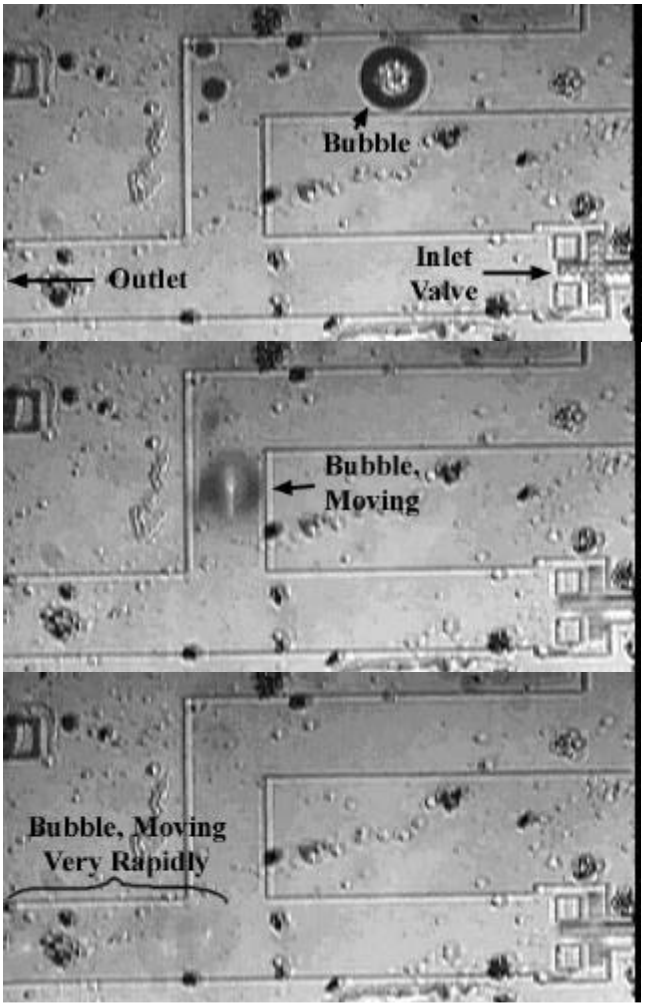

Figure 6. *(Top) Flow channel with a trapped bubble. (Middle) Motion of the bubble after power has been supplied. (Bottom) Acceleration of the bubble as power is maintained.*

As shown in figure 8, when the pump is off, each video frame looks very similar to each other. However, when the pump is on each frame in sequence is quite different from each other. When the heater is on few beads stay in focus for more than 1 frame. When a bead can be seen in more than one frame (which is rare and usually the bead is much more out of focus between frames) a larger displacement can be seen between frames and a linear velocity may be estimated. This implies a much higher flow rate than the background flow and net pumping is observed.

This difference in flow rate is easily apparent on video (at a frame rate of 30 frames per second), but is much more difficult to represent as a series of video frames. When heater power is turned off and the bubble collapses, the initial collapse and pulling on the fluid completely opposes the background flow in the fluid. However, once the bubble is gone, the background flow starts up again. Based on these estimates of flow rate 2 nl of fluid will be delivered for each 5 second cycle leading to a delivery of 1.44 μl/hour if the pumps are operated continuously.

CONCLUSIONS

This work presents a compact MEMS based positive displacement system to deliver drugs off chip. It also represents one of the first integration steps required for a fully autonomous microfluidic system. Microneedles could be integrated with

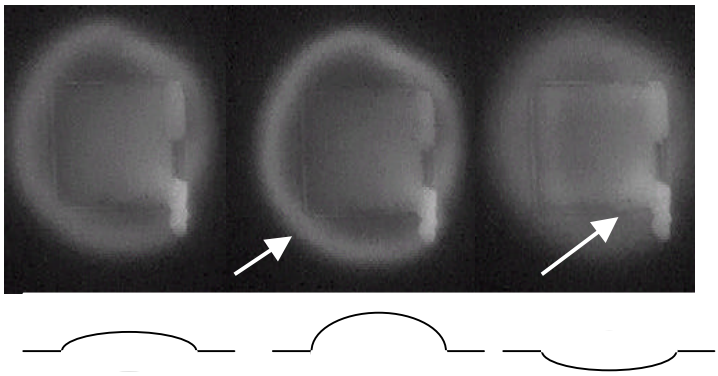

Figure 7. *(Left) Outlet when no bubble is present in the bubble chamber. (Middle) Change in radius of curvature and collection of fluid at the outlet when the pump is actuated. (Right) Change in the radius of curvature when the bubble collapses. Side view of the fluid bubble is shown below the picture*

micromixers as demonstrated in [5]. The system would then be a portable system capable of reconstituting lyophilized drug, and dispensing it at the correct dosage as needed by a patient. The flow rates observed in this study were about an order of magnitude lower than those previously observed in [5] (12.5 nl/sec). This is likely due to an increased resistance to flow from the microneedle. The microneedle contributes more viscous losses to the pump. In addition, the small spacing between the needle and the seat will contribute to a very large drag on the fluid which limits flow rates. A better coupling of the needle to a chip could minimize these losses.

ACKNOWLEDGEMENTS

The authors would like to thank the members of the Liepmann and the Pisano labs for MEMS at the Berkeley Sensor and Actuator Center for technical discussions and assistance. This project has been funded by the DARPA microFLUMES program and by Becton-Dickinson Technologies. All devices were fabricated at the U.C. Berkeley Microfabrication Facilities.

REFERENCES

1. N. Talbot and A.P. Pisano, "Polymolding: Two Wafer Polysilicon Micromolding of Closed Flow Passages for Microneedles and Microfluidic Devices," Proceedings 1998 Solid State Sensor and Actuator Workshop Hilton Head, S.C., pp. 265-268, June 1998.
2. J.D. Zahn, N. Talbot, D. Liepmann and A.P. Pisano, "Microfabricated Polysilicon Microneedles for Minimally Invasive Biomedical Devices," Biomedical Microdevices Vol. (2), Nov. 2000.
3. S. Henry, D.V. McAllister, M. Allen, and M. Prausnitz, "Micromachined Needles for the Transdermal Delivery of Drugs," Proceedings of the IEEE Eleventh Annual International Workshop on MEMS, Heidelberg, Germany, pp. 494-498, January 1998.
4. Bardell, R., Sharma, N.R., Forster, F.K., Afromowitz M.A., and Penny, R. "Designing high-performance micro-pumps based on no-moving-parts valves," Micro-Electrical-Mechanical Systems (MEMS), 1997 ASME International Mechanical Engineering Congress and Exposition, Dallas, TX, DSC-Vol. 234, (1997), pp. 47-53.
5. A.A. Deshmukh, D. Liepmann, and A.P. Pisano, "Continuous Micromixer with Pusatile Micropumps," Proceedings 2000 Solid State Sensor and Actuator Workshop Hilton Head, S.C., pp. 73-76, June 2000.
6. Evans, J.D., Liepmann, D., Pisano, A. P., "Planar Laminar Mixer", MEMS97, Nagoya, Japan, (1997), pp 96-101.
7. A. Papavasiliou, D. Liepmann, and A.P. Pisano, "Fabrication of Free Floating Silicon Gate Valve," Proceedings of the ASME MEMS Division, 1999 IMECE, vol. 1 pp. 435-440.

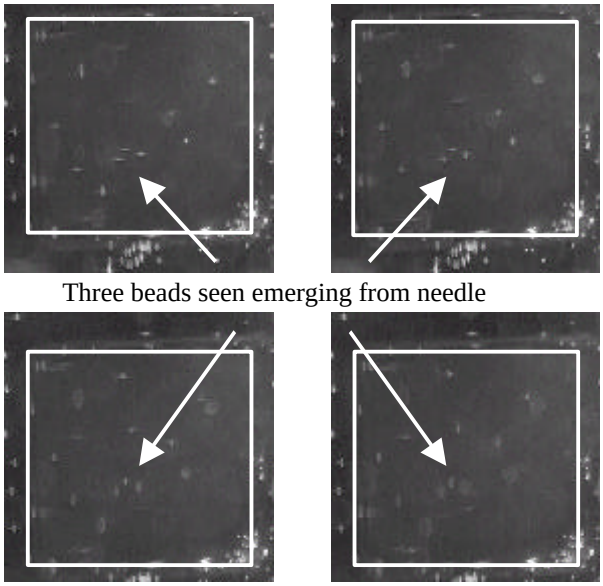

Figure 8. *(Above) a series of four video frames when the pump is off. Notice that beads stay in focus for many frames showing the slow background flow. (Below) a series of four frames once the pump has been turned on. Notice that each frame is dissimilar showing the increased bead velocity and flow rate when the pump is on. One representative bead is tracked, with a large displacement between two frames as indicated by D. The white rectangles indicate the needle outlet.*